Synthesis of quantum dot doped chalcogenide glasses via sol-gel processing

Benjamin Mashford, Julia Baldauf, Tich-Lam Nguyen, Alison M. Funston, and Paul Mulvaney[a)]
School of Chemistry & Bio21 Institute, University of Melbourne, Parkville, Victoria, 3010, Australia

(Received 2 December 2010; accepted 21 March 2011; published online 6 May 2011)

Semiconductor quantum dots (QDs) are used to dope wide-bandgap chalogenide glasses via sol-gel processing. Such chalcogenides enhance surface passivation of the quantum dots, as evidenced by the increased PL emissions of both core and core shell species used, while a ZnO glass leads to irreversible oxidation of the embedded quantum dots. The embedded QDs are photostable. © *2011 American Institute of Physics*. [doi:10.1063/1.3579442]

I. INTRODUCTION

Luminescent materials containing embedded colloidal CdSe-based quantum dot (QD) emitters have applications in a range of fields, including QD light-emitting diodes,[1,2] waveguides.[3,4] solar concentrators,[5] and as optical down-converting filters for GaN-based UV light emitting diodes.[6] An important unresolved problem is related to ensuring that the optimal optical properties of the nanocrystals are preserved upon their introduction into a host matrix. Since the chemical stability and photoluminescence of colloidal QDs are strongly dependent upon their surface chemistry,[7,8] we can expect interactions between the QD and the matrix to critically determine the performance of the nanocomposite. Systems that have been previously studied include QDs embedded into an organic dielectric medium (including PMMA,[6,9] epoxy,[9] and conductive conjugated polymers, e.g., P3HT[10]). The use of polymer host matrices is attractive because they can be processed at low temperatures, thereby leaving the QD ligands largely intact. For applications requiring a higher refractive index (as necessary for waveguiding applications), synthetic routes for embedding QDs into metal-oxide glasses have been developed.[3,4] In the vast majority of these studies, a considerable decrease in the PL yield of the constituent QD component has been reported.

Here, a new approach for forming a host matrix from a large-bandgap inorganic semiconductor is reported. As a matrix material, ZnS is of considerable interest because it has been widely demonstrated to act as an effective surface passivant when it is epitaxially grown onto colloidal CdSe QDs. The concept of embedding CdSe and CdSe/ZnS QDs into a matrix of ZnS might therefore be thought of a logical extension to the formation of a core-shell nanocrystal, with the wide-bandgap matrix playing the role of an additional surface passivating shell layer. As a means of evaluating the advantages offered by a ZnS matrix, we also make a separate set of measurements on QDs embedded in a matrix of ZnO. These experiments enable us to separate out the roles played in maintaining photostability by the dual issues of charge carrier confinement and surface chemistry-related processes.

A fundamental challenge is to homogeneously dope a thin film with nanocrystals with minimal aggregation. This is essential to preserve the size dependent properties of the embedded nanocrystals. As illustrated in Fig. 1, the route taken here to the synthesis of these two nanocomposite systems begins with the preparation of different solutions of mixed colloidal nanocrystals. Each solution contains particles that are stabilized via short-chain ligands and upon spin-coating these solutions onto a smooth substrate, a nanocrystalline thin film is formed. Post-deposition annealing of the films at different temperatures evaporates any remaining solvent and also begins to boil away the volatile short-chain ligands, thus bringing the colloidal nanocrystals into direct contact with one another. An important aspect of the synthesis route developed here is that both the ZnS and ZnO nanocrystals are directly synthesized in polar solvents with short-chain ligands. We propose that this is an important advance because it avoids the laborious extra steps of repeated washing and ligand exchange, which are required when following the traditional synthesis route involving long-chain ligands in high-boiling, relatively nonpolar solvents. Another difference between this and previously described routes to QD-doped metal chalcogenide glasses is that it begins with preformed stoichiometric semiconductor components. The use of preformed colloidal particles allows both lower temperature and oxygen-free annealing. In the traditional sol-gel approach to the formation of a metal-oxide matrix, an air-annealing step is typically used to convert the metal-precursor to its oxide, with the unwanted consequence that the embedded QDs also undergo oxidation.

The size, shape, and ligand chemistry of the ZnO and ZnS materials used in this study are very similar, allowing a direct comparison of the suitability of metal-oxide and metal-sulfide semiconductors as QD host matrices. Since oxygen has a higher electronegativity than sulfur and because oxygen has previously been shown to play an important role in QD photodegradative pathways,[11] we consider the presence of oxygen in the host matrix to be the critical factor that leads to the observed differences in the QD-embedded ZnO and ZnS systems studied here. We report here that optically

[a)]Author to whom correspondence should be addressed. Electronic mail: mulvaney@unimelb.edu.au.

 © 2011 American Institute of Physics

Author complimentary copy. Redistribution subject to AIP license or copyright, see http://jap.aip.org/jap/copyright.jsp

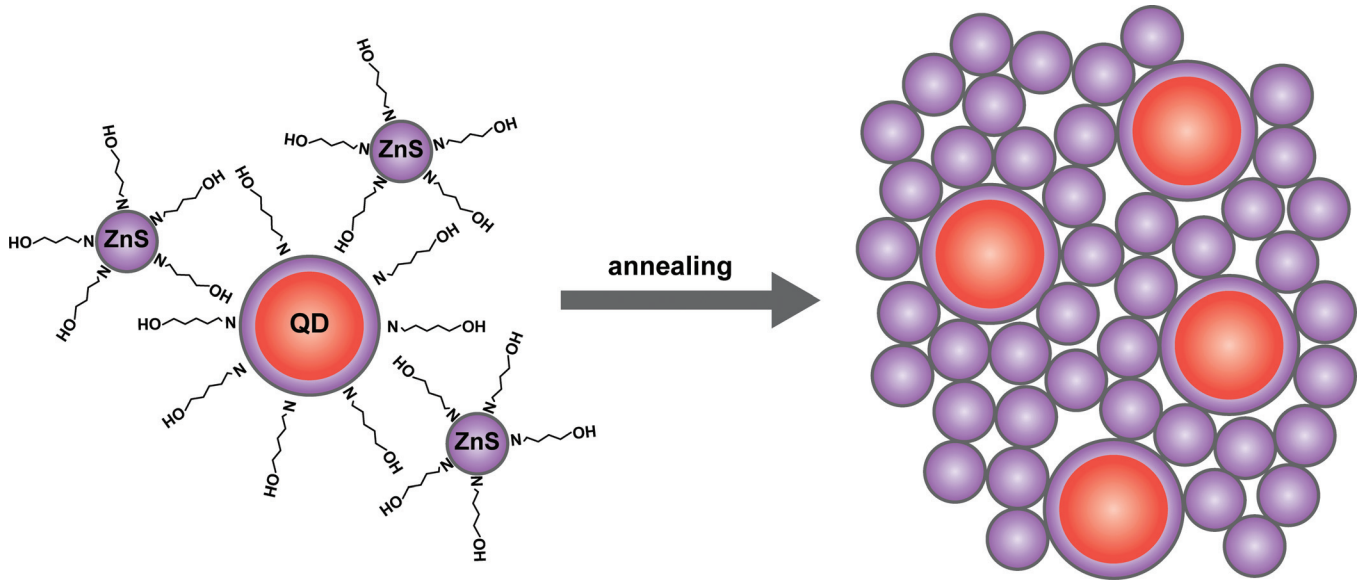

FIG. 1. (Color online) Schematic illustration of the formation of a homogenous dispersion of QDs in a dense nanocrystalline ZnS matrix. The proposed mechanism for formation of the ZnO matrix is identical.

transparent QD-doped semiconductor films of CdSe QDs in ZnS remain highly photostable, suggesting that photodegradation of this chalcogenide-based QD can be kinetically suppressed. Unlike initial reports of QD-doped chalcogenide glasses, which exhibited low photostability and high polydispersity if synthesized *in situ*, these new materials are extremely chemically stable and exhibit high photoluminescence.

II. EXPERIMENTAL PROCEDURE

Zinc acetate dihydrate ($Zn(CH_3COO)_2{\cdot}2H_2O$), tetramethylammonium hydroxide [$(CH_3)_4NOH$, 25% in methanol solution], thioacetamide (CH_3CSNH_2), 4-amino-1-butanol ($H_2N(CH_2)_4OH$) were used as precursor materials without further purification. ZnO nanocrystals were synthesized via a low temperature base catalyzed procedure described in the literature.[12] In a typical reaction, 2×10^{-3} mol of zinc acetate dihydrate was dissolved under stirring into 50 ml of ethanol that was heated to 50 °C. Once fully dissolved, 3×10^{-3} mol of methanolic TMAOH solution was added drop-wise, immediately precipitating ZnO nanocrystals. The solution was stirred for a further 10 min before being removed from the stirring plate and placed in a freezer at −18 °C for storage. For use in further measurements, the nanocrystals were washed via precipitation with ethyl acetate and centifugation before being redispersed into fresh ethanol at 16 times the original concentration. Alcohol-soluble ZnS nanocrystals were synthesized via a new room-temperature synthesis route. In this reaction, 8.2×10^{-4} mol zinc acetate was dissolved while stirring into 12 ml of 1-propanol, along with an equimolar amount of 4-amino-1-butanol. Once fully dissolved, sulfur in the form of 8.2×10^{-4} mol of thioacetamide was added, and the resulting transparent solution was stirred for a further 30 min. ZnS nanocrystals suspended in solution were purified by the addition of ethyl acetate until they precipitated out. The solution was then centrifuged and decanted. The ZnS precipitate was dried under dry nitrogen flow until it formed a transparent gel on the inside of the vial. This was then redissolved into 1-propanol at ten times the original concentration. Separately, CdSe/ZnS core-shell QDs were synthesized by adapting methods recently reported in the literature.[13,14] To render these particles soluble in ethanol, it was necessary to perform a ligand exchange which replaced the original TMPPA and octadecylamine ligand groups with 5-amino-1-pentanol, using a standard ligand-exchange procedure.[4] The QD-to-matrix mass ratio was set at 5 wt. % during the mixing of the two solutions. Photostability tests involved UV irradiation (peak 380–390 nm) at 3 mW/cm^2. Quantum yield (QY) measurements were made with respect to three dyes: rhodamine-6G (QY 0.95 in ethanol[15]), coumarin 153 (QY 0.38 in ethanol[16]), and cresyl violet perchlorate (QY 0.54 in ethanol[17]). All photoluminescence measurements were obtained using a Horiba Fluoro-Log 3 spectrofluorometer. All absorbance spectra were collected with a Cary 5 UV-vis-NIR spectrometer. Single-particle measurements were performed with a home built wide field fluorescence microscope. The QDs were excited with a cw diode laser (470 nm, 100 W/cm^2) and detected with a charge-coupled device camera.

III. RESULTS

Spectroscopic and quantum yield measurements were made on three different sizes of CdSe and three different sizes of CdSe/ZnS colloidal QDs. Each type of QD was then transferred into the ethanol solution before the same set of optical measurements was repeated. The resulting data are summarized in Table I.

As might be expected, the QDs with a passivating ZnS shell exhibit both a higher quantum yield before the ligand exchange, as well as better retention of their QY following re-dispersion into the alcoholic solution. The observed decrease in PL is in agreement with previous reports of a

Author complimentary copy. Redistribution subject to AIP license or copyright, see http://jap.aip.org/jap/copyright.jsp

TABLE I. Summary of relevant parameters for the CdSe and CdSe/ZnS QDs used in this study.

Sample	Emission color	Structure	Solvent	First abs. peak(nm)	Emission peak(nm)	PL QY
C481	blue	CdSe	$CHCl_3$	463	481	0.11
C481E	blue	CdSe	EtOH	461	477	0.01
C540	green	CdSe	$CHCl_3$	526	540	0.17
C540E	green	CdSe	EtOH	523	537	0.07
C632	red	CdSe	$CHCl_3$	623	632	0.15
C632E	red	CdSe	EtOH	622	630	0.05
S493	blue	CdSe/ZnS	$CHCl_3$	472	493	0.25
S493E	blue	CdSe/ZnS	EtOH	472	494	0.25
S545	green	CdSe/ZnS	$CHCl_3$	527	545	0.60
S545E	green	CdSe/ZnS	EtOH	527	544	0.54
S639	red	CdSe/ZnS	$CHCl_3$	621	639	0.37
S639E	red	CdSe/ZnS	EtOH	621	639	0.31

decrease in QD PL emissions when long-chain ligands are exchanged for shorter chain stabilizers.[4]

The transmission electron micrographs in Fig. 2 indicate that reasonably monodisperse particles with a clearly defined crystal lattice have been formed in each of ZnO and ZnS syntheses. The ZnO nanocrystals are measured to be approximately 3–4 nanometers in diameter, while the ZnS are 4–5 nanometers. Analysis of lattice plane spacings allowed both particles types to be indexed to the wurtzite crystal phase.

UV-VIS absorption spectroscopy (Fig. 3) showed that the ZnS nanocrystals exhibit an exciton transition at 270 nm, while the ZnO had a similar absorption profile but with exciton absorption at 330 nm. These wavelengths are considerably blue-shifted from the band-edges of bulk ZnO (385 nm) and ZnS (330 nm) and are therefore indicative of populations of small monodisperse nanocrystals exhibiting quantum-confinement effects.

Measurements of PL emissions from the various solutions were made before and after hotplate stirring. Figure 4 shows that significant increases in PL emissions are observed upon mixing QDs into the ZnS matrix solution, suggesting that significant interactions are already taking place. These interactions are clearly much more pronounced for those systems that involve core CdSe QDs than in those involving CdSe/ZnS core-shell QDs. We attribute this to the ZnS particles acting as a surface passivating agent, in a manner similar to the PL increase that is traditionally observed upon synthetic growth of an epitaxial ZnS shell.

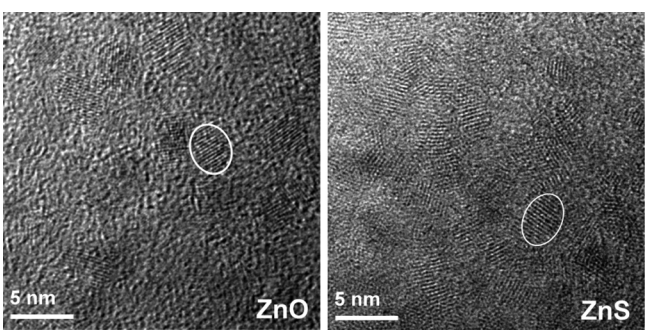

FIG. 2. Transmission electron micrographs of purified ZnO and ZnS nanocrystals.

In comparison, repeating the procedure with the same QDs mixed into a solution of ZnO nanocrystals (see Supplementary Material Ref. 26) led to an immediate decrease in emissions, with a near complete quenching of PL from the core CdSe QDs. These two pieces of data also show a trend that correlate surface interactions to observed optical properties. In each case, the magnitude of change in PL emissions is largest for the blue-emitting (smallest) QDs, followed by the green and then the red QDs. Since smaller particles have a higher fraction of their atoms residing on their surface, these particles will have the highest surface chemistry reactivity.

These varied behaviors of the QD PL in different environments is affirmed by PL traces over time from single S693E QDs in ZnS, air, and ZnO, as shown in Fig. 5. For the single-particle measurements the QD solution was diluted before being mixed with the matrix material, spin-coated onto a glass coverslip, and annealed at 120 °C. The PL of the QDs in the ZnO matrix remains in an off- state most of the time and its on-state is quenched in comparison to the PL of the QD in air. In contrast, the PL of the QDs in the ZnS matrix shows a drastic increase in the on-times and an enhanced PL compared to air. Furthermore, the PL fluctuates mostly

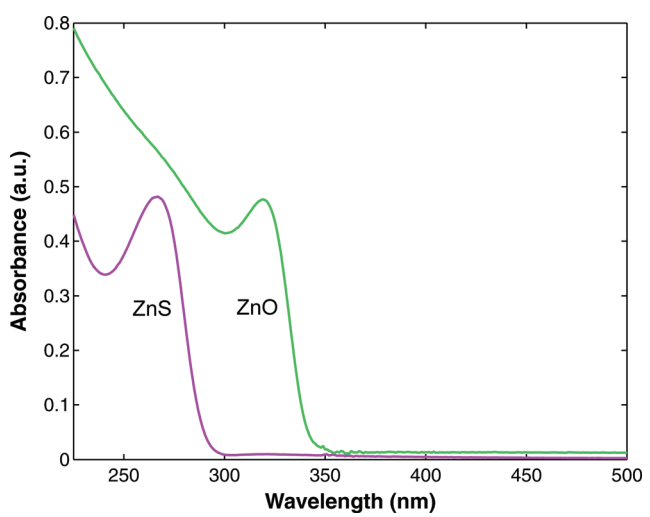

FIG. 3. (Color online) UV-VIS absorption spectrum of ZnO and ZnS nanocrystals dispersed in ethanol solution.

Author complimentary copy. Redistribution subject to AIP license or copyright, see http://jap.aip.org/jap/copyright.jsp

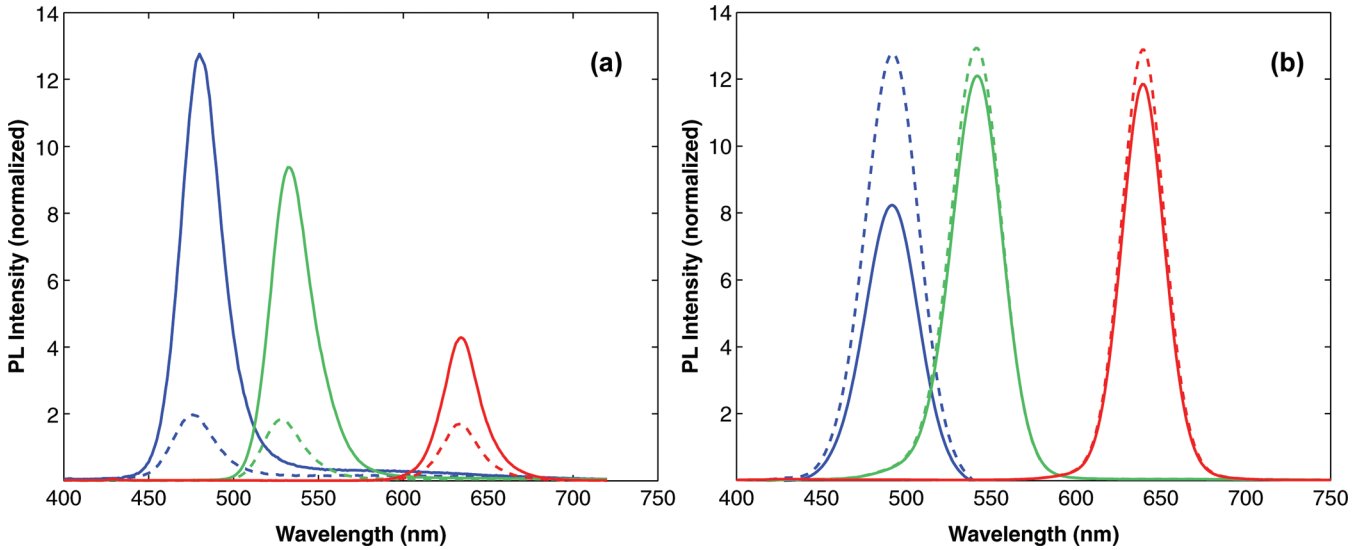

FIG. 4. (Color online) PL spectra of CdSe and CdSe/ZnS QDs mixed into ZnS nanocrystal solutions at 5 wt. % loading. The dashed line is the spectrum measured immediately upon combining the components, while the solid line is that measured after mixing the solution on a hot plate at 60 °C for 5 min. While PL measurements have been normalized, the before/after emission intensities are relative and can be directly compared. The figures represent: (a) core QDs C481E, C540E, and C632E mixed into the ZnS solution, and (b) core-shell QDs S493E, S545E, and S639E mixed into the ZnS solution. An excitation wavelength of 380 nm is used for each measurement.

just between two different intensity states, rather than between an on- and an off-state.

We turn now to measurements of the photostability of the core-shell particles after they have been embedded into the ZnO and ZnS matrices. Illuminating CdSe/ZnS QDs with an excitation energy above their bandgap has been demonstrated to lead to a complicated series of electronic and chemical reactions with the host matrix and/or atmosphere surrounding the particles.[11] In the data shown in Fig. 6, we see a marked difference in the photostability of the ZnO and

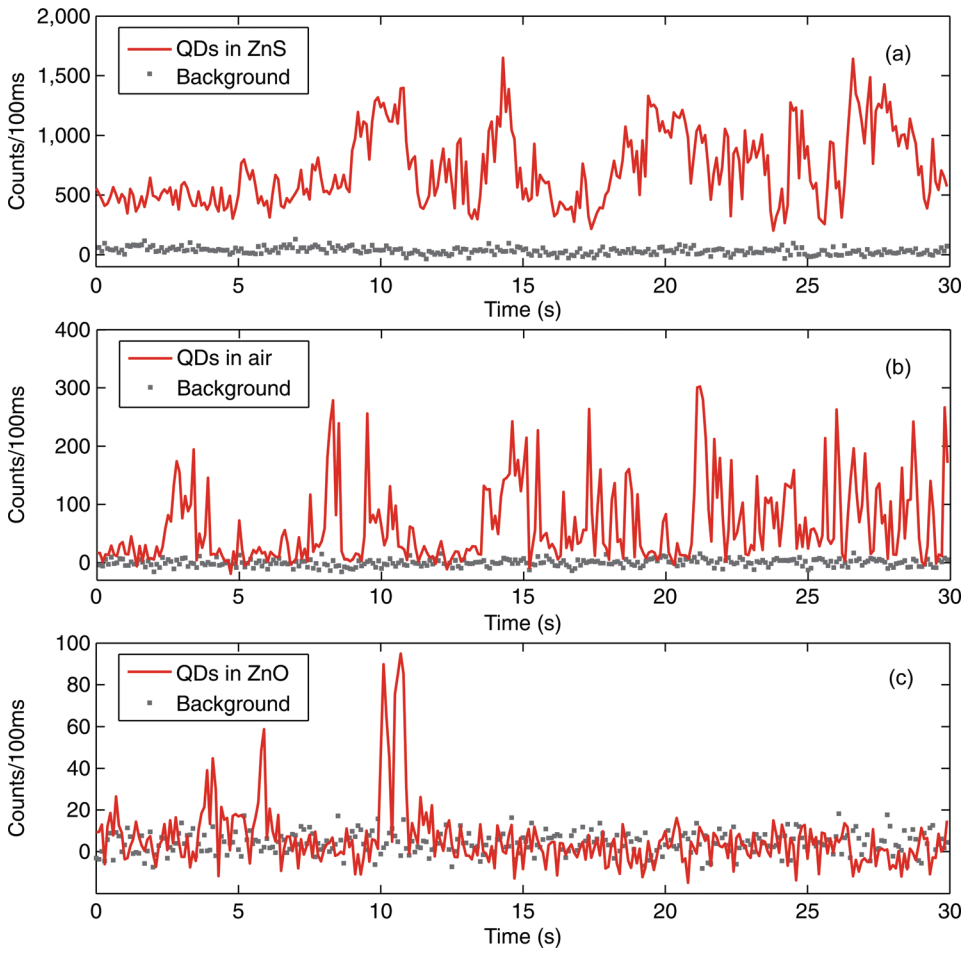

FIG. 5. (Color online) (a) Typical photoluminescence from single S639E QDs in a ZnS matrix, (b) in air, and (c) in a ZnO matrix as a function of measurement time. The PL of QDs in the ZnS matrix show enhanced on-times with two intensity levels in comparison to air, whereas the QDs in ZnO show enhanced off-times.

Author complimentary copy. Redistribution subject to AIP license or copyright, see http://jap.aip.org/jap/copyright.jsp

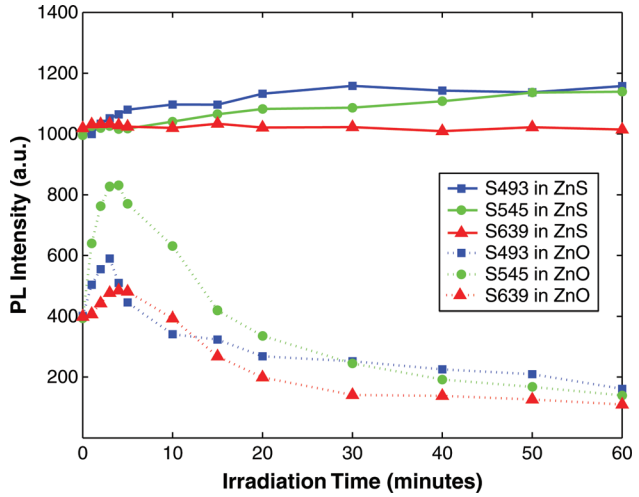

FIG. 6. (Color online) Plot of the PL emission intensity of core-shell QDs dispersed into ZnO and ZnS films as they are exposed to UV irradiation over a period of one hour.

ZnS samples. We attribute this difference to the presence of highly reactive oxygen species in the ZnO matrix. With even a relatively low level of near-UV exposure (3 mW/cm^2) the core-shell QDs in the presence of ZnO undergo photobrightening in the first 5 min of irradiation. This photobrightening is characterized by a temporary increase in PL intensity (as much as 100%) but at longer irradiation times, a steady and monotonic decrease in PL intensity is measured. This decrease is irreversible and is accompanied by a blue-shift in the PL peak position of approximately 5 nanometers, an observation that is in accordance with photo-oxidation. In comparison, emissions from the QDs surrounded by ZnS are very stable over the same measurement period, with only a slight increase in PL emissions being observed. It seems apparent that despite having a thick (4 monolayer) shell of ZnS, the CdSe core is still readily affected by reactions with chemical species in the surrounding environment, with oxygen being the most likely co- reactant. Therefore, in order to attain maximum stability of the QDs, one should aim to achieve complete isolation from the surrounding environment. One approach to this problem is to densify the surrounding matrix via a thermal annealing process. Unlike polymers, inorganic nanocrystalline materials are chemically stable over a wide range of annealing temperatures and various studies have examined the structural changes that nanocrystals undergo as they are sintered together to form a dense, polycrystalline solid.[12,18] Based upon the previous results, the ZnS matrix was chosen for further thermal annealing studies.

Figure 7 illustrates how the absorbance profile of a (non QD-embedded) ZnS film changes as it is heated at different annealing temperatures. A transition is clearly shown from the sharp quantum confined absorbance that is indicative of discrete particles, to a broad shoulder that is typically associated with a bulk semiconductor film. To better understand these structural changes, spectroscopic ellipsometry was employed for measurements of the thickness and refractive index of the ZnS films. As shown in Fig. 7, the ZnS film undergoes large changes in its measured thickness as it is annealed up to 400 °C, reducing to approximately one third of its original value. The porosity of the ZnS film was estimated using an effective medium model

$$\text{Porosity} = \left[\left(\frac{n_d^2 - n_g^2}{n_d^2 + 2n_g^2}\right) \Big/ \left(\frac{n_d^2 - n_g^2}{n_d^2 + 2n_g^2} - \frac{1 - n_g^2}{1 + 2n_g^2}\right)\right] 100\%. \quad (1)$$

The equation relates the measured refractive index of the ZnS thin film ($n_g = 1.7$ at 550 nm at 100 °C, up to $n_g = 1.9$ at 550 nm at 400 °C) to that of bulk crystalline ZnS ($n_d = 2.3$ at 550 nm). The porosity exhibits a less dramatic change than the thickness did, but we must assume that these results integrate the void space due to a distribution of pinholes that appear in all of the samples, as revealed by AFM analysis (see Supplementary Material Ref. 26).

The effect of annealing on the PL emissions from embedded core-shell QDs is shown in Fig. 8(a). In each case, a considerable increase in PL emissions is seen for films that have been annealed in the temperature range of 100–200 °C. At this relatively low annealing temperature, we would not

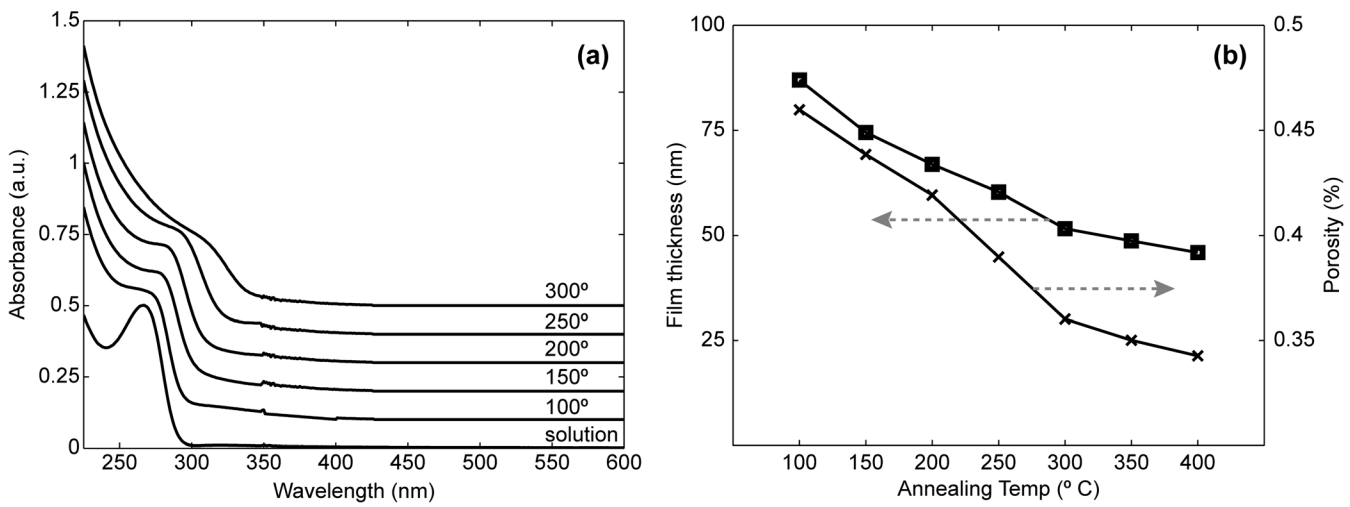

FIG. 7. (a) UV-VIS absorption spectra of ZnS films on quartz substrates that have been processed at different annealing temperatures. The spectra are offset for clarity. (b) Plots of the thickness and estimated porosity of ZnS films that have been processed at different annealing temperatures.

Author complimentary copy. Redistribution subject to AIP license or copyright, see http://jap.aip.org/jap/copyright.jsp

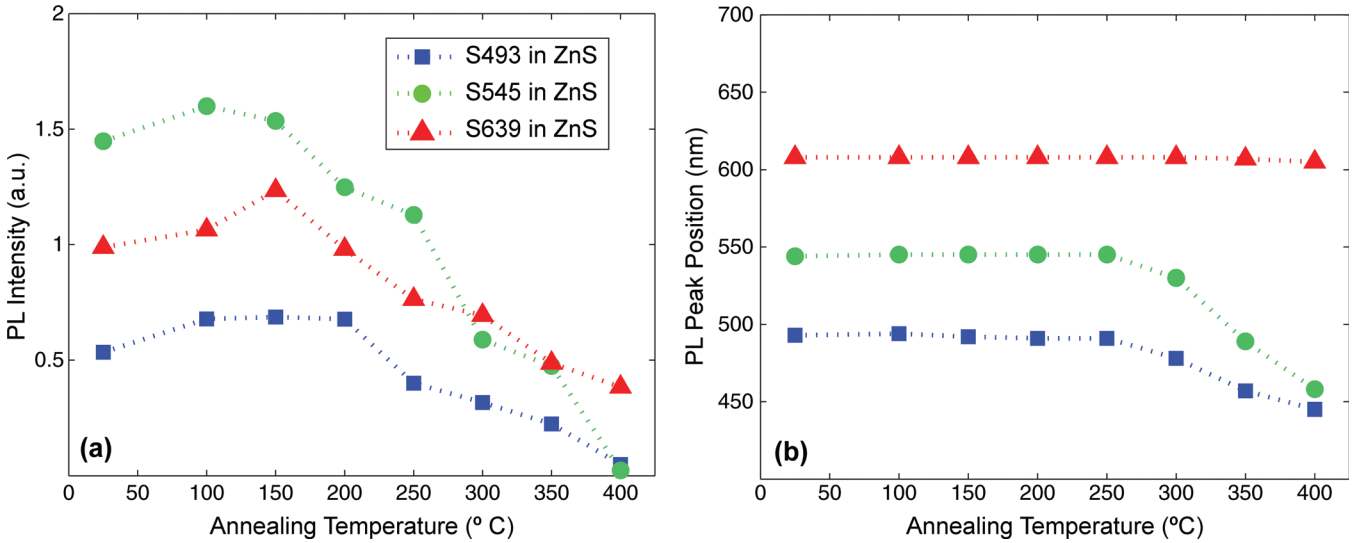

FIG. 8. (Color online) (a) Relative PL emission intensity of CdSe/ZnS QDs dispersed into the ZnS matrix as the film is heated at different annealing temperatures. (b) Peak position of the QD emissions from the same thin film samples at different annealing temperatures.

expect large changes in the phase or morphology of any of the nanocrystal components. This is supported by the minimal shift in the ZnS absorbance peak that was observed at these temperatures [Fig. 7(a)]. Although it is tempting to directly attribute this to the ZnS matrix providing further passivation to the surface of the QDs, it might also more simply be due to thermal annealing of the QDs themselves. Similar results have previously been reported for films of CdTe QDs that have undergone post-deposition annealing.[19] In either case, these results indicate that ZnS provides an environment that is suitable for post-deposition annealing under nitrogen gas. In comparison, similar measurements (not shown) made on the same QDs embedded into a ZnO matrix showed only a steady monotonic decrease with annealing temperature, with very little measurable PL remaining for samples annealed above 200 °C. A plot of the peak position, as shown in Fig. 8(b), shows that no detectable changes in particle size or composition are seen until annealing temperatures are above 250 °C. At this point, the smaller QDs undergo a rapid blue-shift in their PL peak position and we attribute this to the formation of a higher-bandgap alloy as the CdSe core begins to fuse into the surrounding ZnS shell and host matrix. Indeed, it is this effect which may impose a fundamental upper-limit to thermal processing of CdSe QDs.

IV. DISCUSSION

Consider the flat-band diagram in Fig. 9 showing the estimated conduction and valence band levels of the QDs and chalcogenide glass matrix.

The energy levels have been calculated by considering the reported effective masses of electrons and holes in CdSe, ZnS, and ZnO in conjunction with recent literature reports of the ionization energy levels of those materials[20] and clearly predict that CdSe should form a type I interface with the ZnS glass matrix, i.e., that photogenerated electrons and holes remain confined to the QD. Only when the blue-emitting QDs are embedded in a ZnO glass is it likely that a type-II junction is formed, since the QD conduction band is nearly aligned with the ZnO CB energy level. The observed enhancement of the QD PL in the ZnS matrix leads to the conclusion that the ZnS particles act as an "infinite" shell surrounding each QD. The observation of two intensity states at the single particle level supports this statement since two intensity levels were only observed for QDs passivated by a thick CdS shell.[21,22] The passivation of the QD is the key point in order to minimize surface traps that drive the nonradiative decay.[21] This analysis does, however, ignore surface-chemistry related processes that probably play the dominant role in inducing changes in QD PL emissions as they undergo continued photo-excitation over a period of time. For instance, photobrightening of QDs is a process that has been shown to be strongly correlated with the amount of oxygen and/or moisture in the environment surrounding the QDs.[11,23] Oxidation processes have also been linked to observed blue-shifts in QD emission spectra.[24,25] Here, the proposed mechanism is an effective decrease in QD size as the outermost selenium atoms are attacked by oxygen, thus forming the compound SeO_2. The oxidation of the QDs is

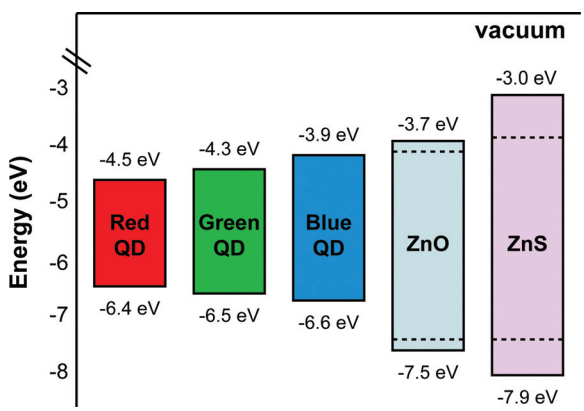

FIG. 9. (Color online) Proposed energy band diagram of the three different-sized CdSe, ZnO, and ZnS nanocrystals used in this study. The dashed lines in the ZnO and ZnS diagrams represent the valence and conduction band energy levels in the bulk forms of these materials.

Author complimentary copy. Redistribution subject to AIP license or copyright, see http://jap.aip.org/jap/copyright.jsp

almost always accompanied by a dramatic decrease in PL emissions, with the strong electron scavenging properties of adsorbed oxygen interfering with the electron-hole recombination process that leads to radiative QD emissions. In the photostability and annealing data presented here, a blue-shift in the emission spectrum is observed whenever a ZnO matrix is used. In each case, this blue-shift is accompanied by lower PL emissions and a decrease that is proportional to the degree of UV exposure. We also conclude that the oxygen source is the ZnO material itself, since no blue-shift is observed in the ZnS matrix case despite all measurements being made in air. Embedding the QDs epitaxially in the chalcogenide material yields passivated QDs and drastically reduces the availability of oxygen and water as redox reagents that can facilitate photo-oxidation.

V. CONCLUSION

The formation of colloidal QDs in a nanocrystalline metal-chalcogenide glass by sol-gel processing has been presented here. The use of short-chain ligands on each nanocrystal component allows a high degree of particle interaction, and this interaction yields immediate and dramatic changes in the optical properties of the embedded QDs. It was found that emissions from CdSe QDs were greatly reduced by their introduction into a ZnO matrix, while they were significantly increased when they were in contact with a ZnS host matrix. Similarly, CdSe/ZnS QDs dispersed into a ZnS matrix showed a much higher level of photostability over that observed in the ZnO matrix samples. It is proposed that this difference in behavior primarily results from the higher degree of chemical reactivity of the oxygen species located in the host matrix, and less importantly on the energy band offsets in the electronic structure of the semiconductor components. For applications requiring stable optoelectronic materials, it is therefore suggested that metal-sulfide components offer significant advantages over metal-oxides for nanocomposite systems containing embedded CdSe QDs. This new synthesis obviates many of the problems beset by the early work in this area to make tunable optical materials.

[1]J. M. Caruge, J. E. Halpert, V. Wood, V. Bulovic, and M. G. Bawendi, Nature Photon. **2**, 247 (2008).
[2]Y. Li, A. Rizzo, R. Cingolani, and G. Gigli, Adv. Mater. **18**(19), 2545 (2006).
[3]J. Jasieniak, J. Pacifico, R. Signorini, A. Chiasera, M. Ferrari, A. Martucci, and P. Mulvaney, Adv. Func. Mater. **17**(10), 1654 (2007).
[4]M. A. Petruska, A. V. Malko, P. M. Voyles, and V. I. Klimov, Adv. Mater. (Weinheim, Ger.) **15**(7–8), 610 (2003).
[5]S. J. Gallagher, B. Norton, and P. C. Eames, Sol. Energy **81**(6), 813 (2007).
[6]H. Song and S. Lee, Nanotechnology **18**(5), 055402/055401 (2007).
[7]C. Bullen and P. Mulvaney, Langmuir **22**(7), 3007 (2006).
[8]S. F. Wuister, A. v. Houselt, C. d. M. Donegáaé, D. Vanmaekelbergh, and A. Meijerink, Angew. Chem. **116**(23), 3091–3095 (2004).
[9]L. Martiradonna, T. Stomeo, L. Carbone, G. Morello, A. Salhi, M. D. Giorgi, R. Cingolani, and M. D. Vittorio, Phys. Status Solidi B **243**(15), 3972–3975 (2006).
[10]K. Palaniappan, J. W. Murphy, N. Khanam, J. Horvath, H. Alshareef, M. Quevedo-Lopez, M. C. Biewer, S. Y. Park, M. J. Kim, B. E. Gnade, and M. C. Stefan, Macromolecules **42**, 3845 (2009).
[11]A. Y. Nazzal, X. Wang, L. Qu, W. Yu, Y. Wang, X. Peng, and M. Xiao, J. Phys. Chem. B **108**(18), 5507 (2004).
[12]C. Czekelius, M. Hilgendorff, L. Spanhel, I. Bedja, M. Lerch, G. Muller, U. Bloeck, D.-S. Su, and M. Giersig, Adv. Mater. (Weinheim, Ger.) **11**(8), 643 (1999).
[13]J. Jasieniak, C. Bullen, J. Van Embden, and P. Mulvaney, J. Phys. Chem. B **109**(44), 20665 (2005).
[14]J. Jasieniak and P. Mulvaney, J. Am. Chem. Soc. **129**(10), 2841 (2007).
[15]R. F. Kubin and A. N. Fletcher, J. Lumin. **27**(4), 455 (1982).
[16]G. A. Reynolds and K. H. Drexhage, Opt. Commun. **13**(3), 222 (1975).
[17]D. Magde, J. H. Brannon, T. L. Cremers, and J. Olmsted, J. Phys. Chem. **83**(6), 696 (1979).
[18]B. Sun, R. L. Peterson, H. Sirringhaus, and K. Mori, J. Phys. Chem. C **111**(51), 18831 (2007).
[19]S. A. Rutledge, A. A. Farah, J. Dinglasan, D. J. Anderson, A. Das, J. Goh, C. Goh, and A. S. Helmy, J. Phys. Chem. C **113**(47), 20208 (2009).
[20]V. Wood, M. J. Panzer, J. E. Halpert, J. M. Caruge, M. G. Bawendi, and V. Bulovic, ACS Nano **3**(11), 3581 (2009).
[21]D. E. Gomez, J. van Embden, P. Mulvaney, M. J. Fernee, and H. Rubinsztein-Dunlop, ACS Nano **3**(8), 2281 (2009).
[22]P. Spinicelli, S. Buil, X. Quelin, B. Mahler, B. Dubertret, and J. P. Hermier, Phys. Rev. Lett. **102**(13), 136801 (2009).
[23]M. Oda, J. Tsukamoto, A. Hasegawa, N. Iwami, K. Nishiura, I. Hagiwara, N. Ando, H. Horiuchi, and T. Tani, J. Lumin. **122–123**, 762–765.
[24]L. Liu, Q. Peng, and Y. Li, Inorg. Chem. **47**(8), 3182 (2008).
[25]M. Oda, A. Hasegawa, N. Iwami, K. Nishiura, N. Ando, A. Nishiyama, H. Horiuchi, and T. Tani, Colloids Surf., B **56**(1–2), 241 (2007).
[26]See supplementary material at http://dx.doi.org/10.1063/1.3579442 for PL emission from CdSe nanocrystals after mixing with ZnS and ZnO solutions and AFM images of the pinholes formed during the annealing of the nanocrystal films.

Author complimentary copy. Redistribution subject to AIP license or copyright, see http://jap.aip.org/jap/copyright.jsp